LBL--15086

DE83 003553 LBL-15086

Conf-820945--6

Lawrence Berkeley Laboratory
UNIVERSITY OF CALIFORNIA

Materials & Molecular Research Division

Presented at the International Ion Beam Modification of Materials '82, Grenoble, France, September 6-10, 1982; and to be published in Nuclear Instruments and Methods

THE EFFECT OF RECOILED O ON DAMAGE REGROWTH AND ELECTRICAL PROPERTIES OF THROUGH-OXIDE IMPLANTED Si

D.K. Sadana, N.R. Wu, J. Washburn, M. Current, A. Morgan, D. Reed, and M. Maenpaa

October 1982

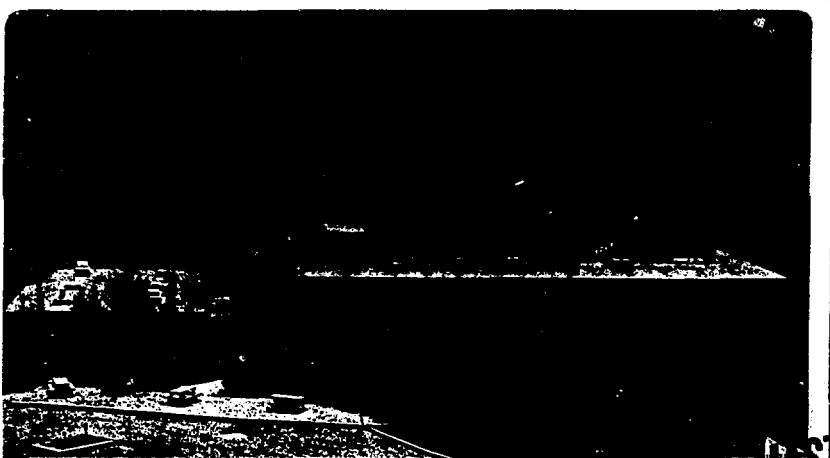

Prepared for the U.S. Department of Energy under Contract DE-AC03-76SF00098

THE EFFECT OF RECOILED O ON DAMAGE REGROWTH AND ELECTRICAL PROPERTIES OF THROUGH-OXIDE IMPLANTED Si

D.K. Sadana, N.R. Wu and J. Washburn
Lawrence Berkeley Laboratory, University of California, Berkeley, CA
M. Current* and A. Morgan
Philips Research Labs, Signetics Corporation, Sunnyvale, CA
D. Reed
University of Illinois, Champagne, Urbana, IL
M. Maenpaa
California Institute of Technology, Pasadena, CA

ABSTRACT

High dose (4-7.5 x 10^{15} cm^{-2}) As implantations into p-type (100) Si have been carried out through a screen-oxide of thicknesses $\leq$775Å and without screen oxide. The effect of recoiled O on damage annealing and electrical properties of the implanted layers has been investigated using a combination of the following techniques: TEM, RBS/MeV He^+ channeling, SIMS and Hall measurements in conjunction with chemical stripping and sheet resistivity measurements. The TEM results show that there is a dramatically different annealing behavior of the implantation damage for the through oxide implants (Case I) as compared to implants into bare silicon (Case II). Comparison of the structural defect profiles with O distributions obtained by SIMS demonstrated that retardation in the secondary damage growth in Case I can be directly related with the presence of O. Weak-beam TEM showed that a high density of fine defect clusters ($\leq$50Å) were present both in Case I and Case II. The electrical profiles showed only 30 percent of the total As to be electrically active. The structural and electrical results have been explained by a model that entails As-O, Si-O and As-As complex formation and their interaction with the dislocations.

* Now at Trilogy Systems Corp., Cupertino, CA 95014

INTRODUCTION

Implants through thin dielectric layers (oxides and nitrides) are common features of IC device processing (1). The principal advantages of this procedure over implanting directly into bare Si include: (a) process simplicity and implant depth modulation (2,3), (b) protection of device areas from contamination from sputtered material during implanting (4) and (c) improved control on device parameters such as leakage currents (1,5) and gettering efficiency (6).

For implants where the peak of the profile is at a depth comparable to the dielectric layer thickness, copious quantities of atoms from the screen layer are "recoil implanted" into the substrate region (7,8). Monte Carlo (9) and analytical (10-12) methods have been applied to the calculation of the number of oxygen atoms which are recoil-implanted into Si for implants through thin oxide layers. Application of Boltzmann transport equation methods (12) has predicted recoil yield and oxygen depth profiles which have been experimentally verified in this study and by others (13).

For a high dose (10^{15} ions cm^{-2}) through a screen oxide, the concentration of recoil implanted oxygen at the oxide interface can be greater than 10^{21} oxygen atoms cm^{-3}. The presence of these high levels of oxygen (~10^3 times higher than oxygen solubility limits at ~1200°C), has a profound effect on the nature and density of lattice defects present after high temperature annealing (14-15). A strong pinning effect on dislocation loops from recoil implanted oxygen (17) was observed in this study for anneals in N_2 and oxidizing ambients.

Comparative studies of the residual defects and electrical properties of annealed implants through screen oxides have also indicated significant differences between Si of (100) and (111) orientations (18).

EXPERIMENTAL

The experimental program was designed to be comparable to the general processing conditions of an all-implanted, MOS device fabrication technology. The specific implants discussed in this paper were processed with simplified "standard" conditons. The wafer material was p-Si(100), 7-33 ohm-cm Boron doped. All wafers were oxidized before implantation to the full oxide thickness. Thinner screen oxides and "bare Si" conditions were obtained by controlled etching in a buffered oxide etch. In this way, all wafers were subjected to similar thermal processing (initial oxidation at 950°C and post-implant anneals).

The implants were done with As ion beams of 4 to 12 mA for doses of 4 to 7×10^{15} As^+ cm^{-2} at 100 and 120 keV. The wafers were either "bare Si" or with oxides of 300, 475, or 775 Å. The principal anneal cycle used in this study was 30 minutes in N_2 at 1000°C. Additional tests were done for annealing temperatures between 700 and 1050°C as well as annealing at 1000°C in oxidizing ambients with HCl of 0, 3 or 10 percent.

The analytical techniques employed include extensive use of TEM (in plan and cross-section (XTEM)), RBS (with 1.5 MeV He^+ beams in channeled or random orientation) and SIMS (Ar^+ and Cs^+ beams with a Cameca 3F system). Electrical characterization was done with surface

sheet resistance measurements with a four-point probe (19) and Hall mobility and carrier concentration measurements done in conjunction with anodic etching depth profiling.

RESULTS

A. Pinning of Structural Defects by O

The TEM cross-section (XTEM) micrographs from the samples that were implanted through 30Å ("bare-Si"), 475Å and 775Å screen oxides, all showed continuous amorphous layers extending from the SiO_2/Si interfaces with progressively decreasing widths being 1050Å, 1000Å, and 680Å, respectively. This was expected from the reduced range of As atoms in the Si substrate with thicker screen oxides. The thickness of 775Å correspond to the projected range of As in SiO_2 at 120 kev and therefore only about 50 percent of the As atoms penetrated the Si in this case. The As distributions obtained by both RBS and SIMS from these samples showed approximately gaussian distributions. The XTEM micrographs and atomic distributions from some of the samples have been reported earlier (17).

Figures 1a, b, and c, show weak-beam TEM plan view micrographs from the samples described above after annealing them at 1000°C for 1/2 hour in N_2 (with ramp up from 500°C and ramp down to 900°C). The corresponding cross-section micrographs (bright-field TEM) are shown in Figs. 2a, 3a and 4a, respectively. It is clear from these results that the amorphous layers have recrystallized by solid phase epitaxy on the undamaged Si substrate. In the bare Si case, the residual lattice defects are in the form of dislocation half-loops

which intersect the surface of the bare Si and extend several thousand Angstroms into the wafer. This type of lattice defect structure has been discussed many times in the literature (15,17). In the case of thorough-oxide implantation, the defects were localized into discrete layers (Figs. 3a and 4a). The XTEM results from the 475Å and 775Å screen-oxide samples are similar in that well defined dense layers of dislocation loops form at depths which are slightly deeper than the amorphous/crystalline interface present immediately after high dose implantation. In addition, small defect clusters were present in the near surface region (0-250Å) of these samples. In the 475Å case there was an extra layer of small dislocation loops (350Å across, Fig. 2a) between the surface and the deeper dense layer of dislocations.

The oxygen distributions (Figs. 2b, 3b, and 4b) before and after the annealing were obtained by SIMS and the results are directly compared with structural defects distributions from the XTEM micrographs (Figs. 2, 3 and 4). It is clear from these results that the positions of the layers densely populated with dislocation loops matches precisely with the peaks in the O profiles after annealing. Similar association of O with defects has been speculated in results reported recently although direct correlation with discrete defect layers was lacking (1,5,7).

B. As, Carrier Concentration Profiles

Figure 5 shows the As and carrier concentration profiles from the annealed samples in which As was implanted through 30 Å (bare), 475 Å and 775Å screen oxides. For comparison, As distributions in the un-

annealed samples have also been included. No local peaks (20) in the atomic As distributions were observed for the annealed material. The broad plateau with concentrations 2-3x10^{20} cm^{-3} over the depth ranges 0-0.3μm followed by a sharp decline was in agreement with earlier results (21). The As spectra obtained in a channeling direction by RBS indicated that a large fraction (~50 percent) of the atoms were located in non-substitutional positions. The non-substitutional As distribution did show a peak at ~1000Å for the 775 Å screen oxide case which correlates well with the position of the layer of dislocation loops in Fig. 4a (23). The metallurgical junction depths varied with oxide thickness from 0.25 to 0.4μm. The results of structural studies, atomic profiles and junction depths as a function of screen-oxide thickness are summarized in Fig. 6.

Comparison of As and carrier concentration profiles show that only 30-40 percent of the As is electrically active (22). The average mobilities in the depth range 0-2000Å were ~600-800cm^2/volt-sec and were in general agreement with high concentration mobilities in Si.

C. Effect of Annealing Ambient on Defects Formation

A summary of the results of the annealing behavior of the amorphous layers in bare and through oxide (~300Å) implanted (100) Si in various ambients, such as, N_2, O_2 and N_2+O_2+HCl and their combinations is given in Table 1. The TEM micrographs in this study were taken under weak-beam diffraction conditions using a 220 type g vector (micrographs not included in the text). The implantation conditions discussed in this section were 100 keV and a dose of 5 x 10^{15} cm^{-2}.

The As implants were done with an AIT-IIIX implanter using a beam current of 12 mA. The following points were noted while comparing the results of bare and through-oxide cases listed in Table 1. (1) More restricted growth of defects (dislocation loops or networks) occurred in the case of thorough-oxide implants as compared to the bare implants, irrespective of the ambient used, (2) the annealing out of the defects in both cases accelerated in the presence of O_2 or O_2+HCl ambient, (3) the addition of HCl up to 10 percent in O_2 did not significantly enhance the annealing out of the defects, as compared to that obtained by O_2 only, and (4) all of the samples (bare and through-oxide) contained a high density of fine defect clusters in the background under all annealing conditions. These defect clusters were not easily detectable under bright-field diffraction conditions and therefore have not been considered in the bare implanted Si in the previously published literature (1).

DISCUSSION

It is clear from these results that several types of secondary defects originate during annealng: fine defect clusters, straight a/2 <110> dislocation lines running very close to the surface, small dislocation loops, large half loops of dislocations intersecting the surface and dislocation networks. In most of the samples, two or three of these types of defects were present, in addition, the fine defect clusters (<50 Å) were present in all cases. Figures 1b and 1c also show that the shapes of the dislocation loops are quite irregular, indicating that dislocations are interacting with fine scale defect clusters.

Comparison of the recoiled-oxygen curves from the unannealed and annealed samples indicate that some of the O is lost in the annealing process. Since it has been shown that the redistribution of O can occur at temperatures as low as 450°C (13), it is expected that O would diffuse interstitially both toward the surface and deeper into the material in the early stages of high temperature annealing. The local peak of O should therefore form by gettering of O to the layer of dislocation loops that begin to nucleate at 500-550°C. The O atoms are expected to react chemically with Si during the annealing to form stable SiO_x complexes which appear as fine defect clusters in Fig. 1 and restrict the growth of the dislocation loops. The gettering of O to the loops is confirmed by the results of Figs. 3 and 4 where the two different thicknesses of the screen-oxide, the dense layers of the dislocation loops nucleated at different depths from the SiO_2/Si interface and the positions of the O peaks also shifted accordingly.

During the annealing of the implanted Si in an O_2 atmosphere, the following dynamic events are expected to be in progress: 1) The oxidation of Si at the surface which releases Si intersitials into the wafer (24). 2) As at the the SiO_2/Si interface is being pushed into the material because of its low solubility in SiO_2 (the so called snow-ploughing effect) (25). 3) The implantation induced amorphous layer regions regrow and the large number of As and Si interstitials within the implanted region precipitate to form dislocation lines and loops. 4) In the case of the through-oxide implant, the recoiled

oxygen is expected to interact with the Si interstitials and nucleate Si-O complexes (19). 5) Additionally, because of the high dose of As, As precipitation may occur (26). The presence of the fine defect clusters in all the samples studied suggests that the clusters are not just Si-O complexes, but also involve As. A number of different defect clusters, consisting of As-As or As-Si complexes in the bare implanted Si and As-O, As-Si-O in the through oxide implanted are possible. The involvement of O in clustering is supported by the results of Figs. 2, 3, and 4, while As clustering is indicated by the electrical and MeV He^+ channeling measurements. However, the precise composition of these defect clusters is unknown.

For the implant and anneal conditions used in this study, the major defect structures are located at depths less than half of the junction depth, particularly for the screen oxide implants. The contributions of defect penetration of the active junction along the vertical direction to junction leakage in MOS capacitor sturctures were found to be minimal (5,17). The effect of the fine defect clusters near the surface on leakage current is not yet clear.

CONCLUSIONS

The major findings of this study are:

1. Differences in nature and location of residual defects were seen for As implants into bare Si compared to through screen oxides of 500 to 800 Å. Pinning of dislocation loops by oxygen recoil-implant occurred in the through-oxide implanted case.

2. Local segregation of oxygen was observed by SIMS at depths corresponding to residual defect layers (observed by XTEM and channeld RBS).
3. High densities of small (<50Å) defect clusters were observed by weak-beam TEM. These may be associated with As and oxygen complexes with silicon.
4. Systematic variation in junction depths and location of defect layers with oxide layer thickness at 120 kev are consistent with the depth of penetration of As and oxygen into the Si.

ACKNOWLEDGMENTS

The authors would like to thank John Macro and Howard Huff for encouragement and general assistance during the course of this work. We acknowledge the financial support by the Director, Office of Energy Research, Office of Basic Energy Sciences, Materials Sciences Division of the U.S. Department of Energy under Contract No. DE-AC03-76SF00098. and Signetics Corporation, Philips Research Laboratories, Sunnyvale, CA.

Table 1.

Ambients (Annealing at 1000°C)	As → (100) Si t_{ox} = 30Å t_{ox}	Structural Defects Data	R Ω/□	t_{ox} after annealing (Å)	As → SiO_2/(100) Si t_{ox} = 300Å Structural Defects Data	R Ω/□
N_2 (1/2 hr)	34	low density of big loops (2000Å), some dislocation lines, fine defect clusters	29.82	218	entangled dislocations, fine defect clusters and small dislocation loops (~500Å)	32.71
N_2 (1/2 hr) + N_2 (1/2 hr)	40	Same as No. 1 but with fewer loops and dislocation lines, fine defect clusters	25.37	259	two sets of dislocation 1st set 500-1000Å, IInd set ≤200Å; fine defect clusters	27.84
N_2 (1/2 hr) + O_2 (1/2 hr)	579	a/2 <110> straight dislo-tions, fine defects	27.09	698	small dislocation loops (~500Å), high density of fine defect clusters	33.27
O_2 (1/2 hr)	643	same as No. 3	30.41	692	a dislocation network, fine defect clusters	34.71
O_2 + 10 HCl (1/2 hr)	1791	same as No. 3	34.82	1005	same as No. 3 but fewer fine defect clusters	34.71
N_2 + O_2 + 10 HCl (1/2 hr)	1375	fine defect cluters no dislocations	30.33	993	same as No. 3 but fewer fine defect clusters	29.97

REFERENCES

1. H. J. Geipel and R. B. Shasteen, IBM J. Res. Develop., 24, 362 (1980).

2. T. Hirao, K. Inoue, Y. Yaegashi and S. Takayanagi, Japanese J. Appl. Phys. 18, 647 (1979).

3. T. Hirao, G. Fuse, K. Inoue, S. Takayanagi, Y. Yaegashi and S. Ichikawa, J. Appl. Phys. 50, 5251 (1979).

4. E. W. Haas, H. Glawischnig, G. Lichti and A. Blier, J. Electronic Materials, 7, 525 (1978).

5. Y. Wada and N. Hashimoto, J. Electrochem. Soc., 127, 461 (1980).

6. H. J. Geipel and W. K. Tice, IBM J. Res. Develop. 24, 310 (1980).

7. R. A. Moline and A. G. Cullis, Appl. Phys. Lett., 26, 551 (1975).

8. T. Hirao, K. Inoue, S. Takayanagi and Y Yaegashi, Appl. Phys. Lett., 31, 505 (1977).

9. N. Natsuaki, M. Tamura and T. Tokuyama, Japanese J. Appl. Phys. 15, 2427 (1976).

10. R. A. Moline, G. W. Reutlinger and J. C. North, "Atomic Collisions in Solids," Vol. 1., eds. S. Datz, B. R. Appleton and C. D. Moak (Plenum, New York, 1975), p. 59.

11. B. Villepelt, F. Ferrieu, A. Grouillet, A. Golański, J. P. Galliard and E. Ligeon, Nuc. Inst. Meth. 182/183, 137 (1981).

12. L. A. Christel, J. F. Gibbons and S. Mylroie, Nuc. Inst. Meth. 182/183, 187 (1981).

13. T. J. Magee, C. Leung, H. Kawayoshi, L. J. Palkuti, B. K. Furman, C. A. Evans, L. A. Christel, J. F. Gibbons and D. S. Day, Appl. Phys. Lett. 39, 564 (1981).

14. W. K. Chu, H. Muller, J. W. Mayer and T. W. Sigmon, Appl. Phys. Lett. 25, 297 (1974).

15. S. Mader and A. E. Michel, J. Vac. Sci. Technol., 13, 391 (1976).

16. N. Natsuaki, M. Tamura, M. Miyao and T. Tokuyama, Japanese J. Appl. Phys. 16, Suppl. 16-1, 47 (1977).

17. D. K. Sadana, J. Washburn, M. Stratiman, M. Current and M. Maenpaa, Inst. Phys. Conf. Ser. (London) No. 60, 453 (1981).

18. T. Izumi, T. Matsumori, T. Hirao, Y. Yaegashi, G. Huse and K. Inoue, Nuc. Inst. Meth, 182/183, 483 (1981).

19. D. S. Perloff, J. Electrochem. Soc. 123, 1745 (1976).

20. A. Yen, J. Vac. Sci. Technol. 18, 895 (1981).

21. R. Fair and J. Tsai, J. Electrochem. Soc. 122, 1689 (1975).

22. R. Fair, Electrochem Soc. Proc. 81(5), 963 (1981).

23. M. C. Current and D. K. Sadana, unpublished.

24. R. Deal, Electrochem. Soc. Proc. (Semiconductor Technology), 82(5), 15 (1982).

25. H. Muller, J. Gyulai, W. K. Chu, and J. W. Mayer and T. W. Sigmon, J. Electrochem Soc. 122, 1234 (1975).

26. G. J. Van Gurp, J. W. Slotboom, F. J. B. Smolders, W. T. Stacy and Y. Tamminga, J. Electrochem. Soc. 127, 1813 (1980).

27. R. Fair, J. App. Phys. 43 1278 (1972).

FIGURES

Figure 1. Weak-beam plan-view TEM micrographs in a (220) type reflection showing fine defect clusters and pinned dislocation loops (a) t_{ox} = 30Å, (b) t_{ox} = 475Å and (c) t_{ox} = 775Å.

Figure 2. Comparisons of (a) the structural-defects profile (XTEM) with (b) O profile (SIMS). No local O peak occur for t_{ox} = 30Å (bare Si).

Figure 3. Comparison of (a) the structural-defect profile (XTEM) with (b) O profile (SIMS). Local segregation of O occurs at the densely populated layer of dislocation loops (t_{ox} = 475Å).

Figure 4. Comparison of (a) the structural-defects profile (XTEM) with (b) O profile (SIMS). Local segregation of O occurs at the layer of dislocation loops (t_{ox} = 775Å).

Figure 5. Comparison between As and carrier concentration profiles (a) t_{ox} = 30Å, (b) t_{ox} = 475Å, and (c) t_{ox} = 775Å.

Figure 6. Defects location and junction depth as a function of screen-oxide thickness. Line labeled R Fair (1972) (ref. 27) shows the junction depths of As capsuled diffusion.

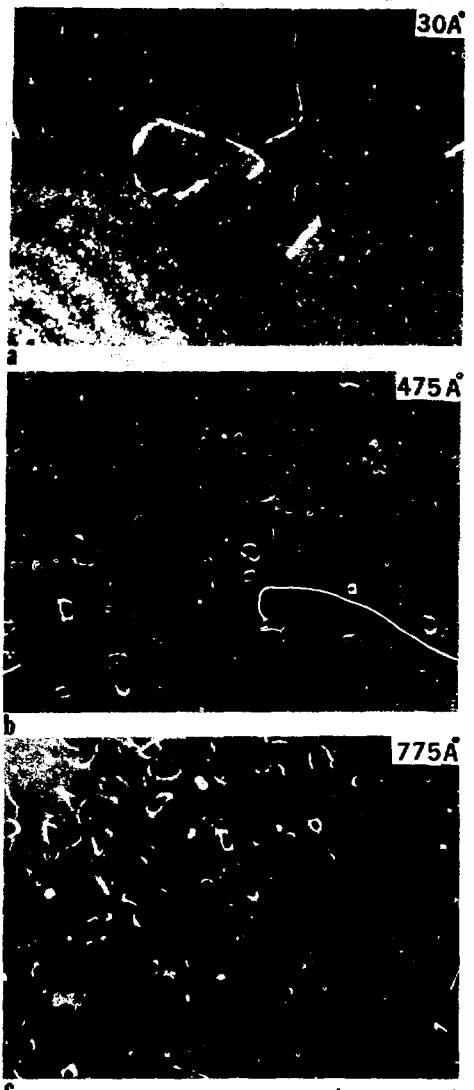

Fig. 1

XBB 828-7367

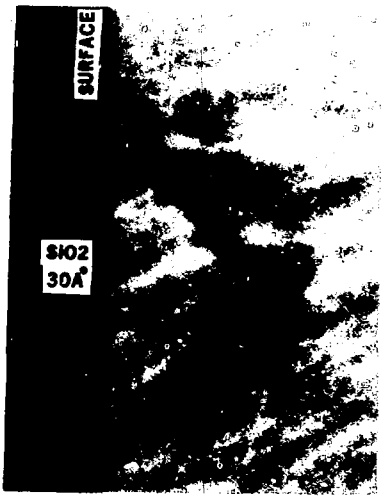

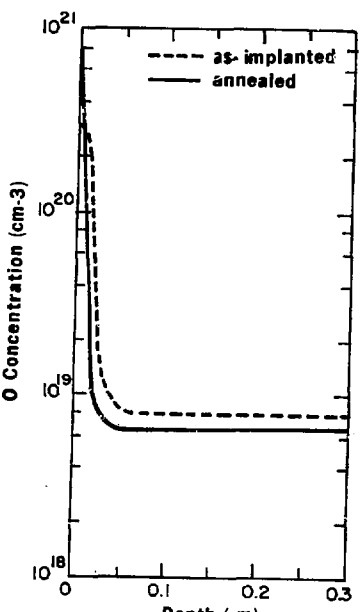

Fig. 2

XBB 828-7443

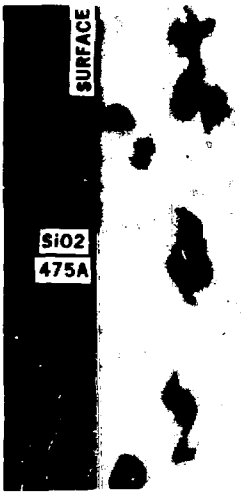

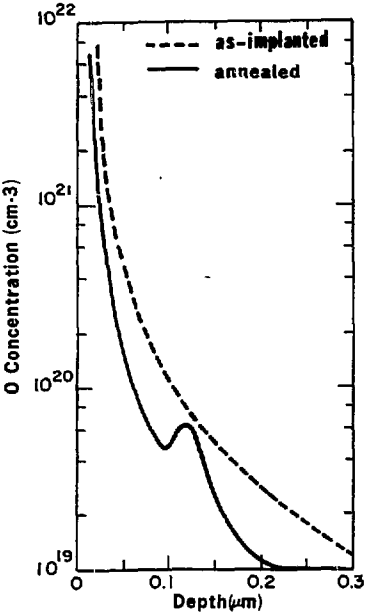

Fig. 3 XBB 828-7445

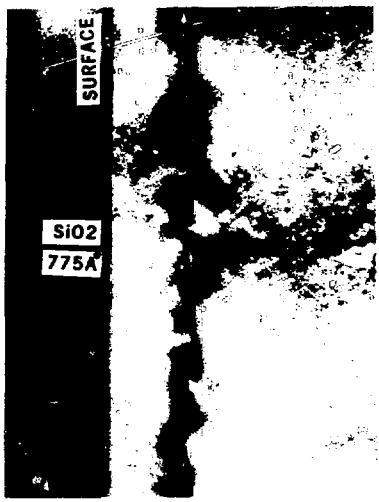

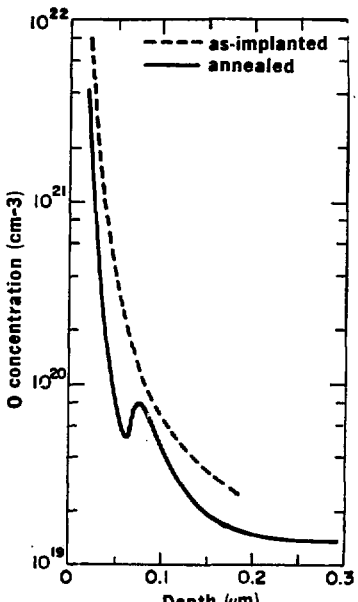

Fig. 4 XBB 828-7444

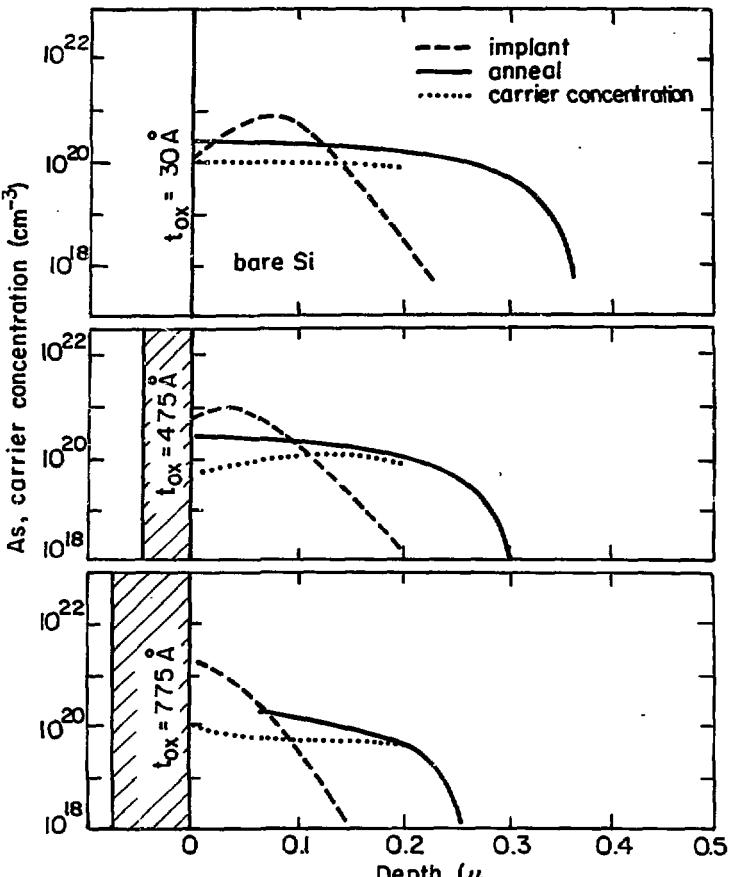

Fig. 5

XBL828-6418

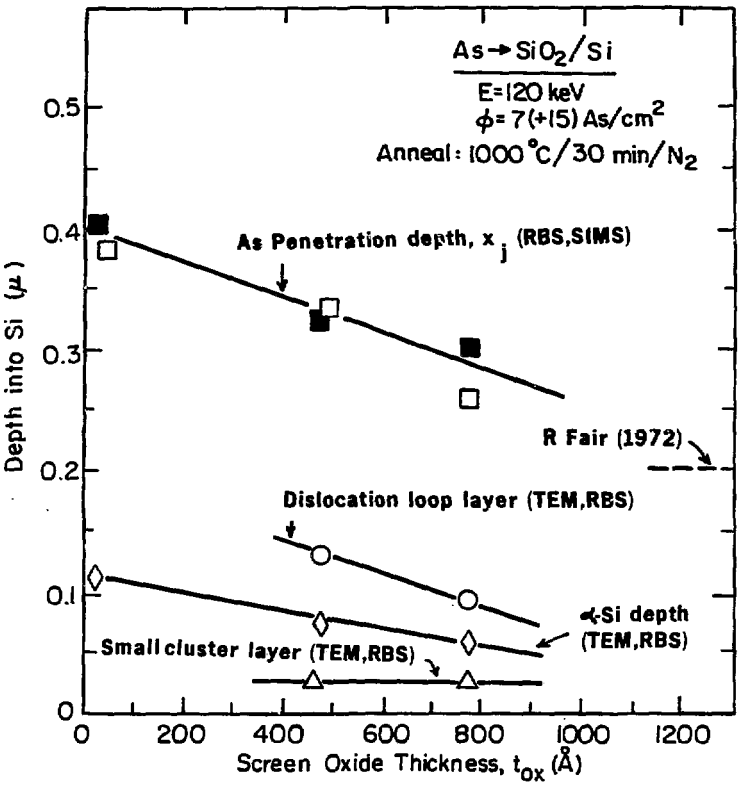

Fig. 6

XBL 828-6419